Accepted Manuscript

Title: Biocompatible and fluorescent superparamagnetic iron oxide nanoparticles with superior magnetic properties coated with charged polysaccharide derivatives

Author: Dorota Lachowicz Agnieszka Szpak Katarzyna Małek-Ziętek Mariusz Kępczyński Robert N. Muller Sophie Laurent Maria Nowakowska Szczepan Zapotoczny

Biocompatible and fluorescent superparamagnetic iron oxide nanoparticles with superior magnetic properties coated with charged polysaccharide derivatives

Dorota Lachowicz,[†,‡] Agnieszka Szpak,[†] Katarzyna Małek-Ziętek,[#] Mariusz Kępczyński,[†] Robert N. Muller,[§,∫] Sophie Laurent,[§,∫] Maria Nowakowska,[†,*] Szczepan Zapotoczny[†,*]

[†]*Faculty of Chemistry, Jagiellonian University, Ingardena 3, 30-060 Krakow, Poland*

[‡] *Academic Centre of Materials and Nanotechnology, AGH - University of Science and Technology, Kawiory 30, 30-055 Krakow, Poland*

[#] *M. Smoluchowski Institute of Physics, Faculty of Physics, Astronomy and Applied Computer Science, Jagiellonian University, Łojasiewicza 11, 30-348 Krakow, Poland.*

[§]*Department of General, Organic and Biomedical Chemistry, NMR and Molecular Imaging Laboratory, University of Mons, Avenue Maistriau, 19, B-7000 Mons, Belgium*

[∫] *Center for Microscopy and Molecular Imaging (CMMI), Rue A. Bolland, 8, 6041Gosselies, Belgium*

Corresponding authors: email: zapotocz@chemia.uj.edu.pl

email: nowakows@chemia.uj.edu.pl

Graphical abstract

SPION-CCh(+) HA-CUR SPION-CCh(+)-HA-CUR(-)

SPION (SuperParamagnetic Iron Oxide Nanoparticle)

Confocal image of cells after treatment with SPION-CCh(+)-HA-Cur(-)
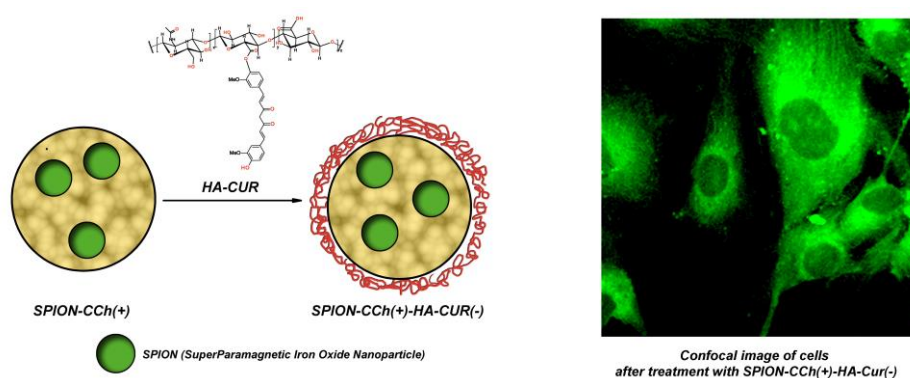
Highlights:

- superparamagnetic iron oxide nanoparticles labeled with cumarine were synthesized
- nanoparticels exhibit superior magnetic properties as contrast agents for MRI
- they easily penetrate cell membrans and can be tracked by fluorescencje microscopy
- they were shown to be non-toxic due to hyaluronic acid coating

Abstract:

Syntheses and characterizations of biocompatible superparamagnetic iron oxide nanoparticles with embedded curcumin and coated with ultrathin layer of hyaluronic acid-curcumin (HA-Cur) conjugate have been reported. Zeta potential measurements confirmed effective coating of native iron oxide nanoparticles stabilized by cationic derivative of chitosan (SPION-CCh) with the synthesized HA-Cur conjugate. Both SPIONs with embedded curcumin and the ones coated with HA-Cur (SPION-CCh/HA-Cur) revealed desired magnetic characteristics while fluorescent properties were much better for the coated nanoparticles. SPION-CCh/HA-Cur nanoparticles were shown to be very promising candidates for T_2 MRI contrast agents as they can easily penetrate cell membrane and their relaxivity is exceptionally high (ca. 470 mM^{-1}·s^{-1}). They may be also tracked using confocal fluorescence microscopy due to the presence of fluorescent curcumin in the coating. *In vitro* studies indicated that the obtained SPIONs-CCh/HA-Cur were non-toxic for EA.hy926 endothelial cells.

Keywords: SPION, cationic chitosan, hyaluronic acid, curcumin, nanoparticles

1. Introduction

Superparamagnetic iron oxide nanoparticles (SPION) are small, crystalline particles made commonly of γ-Fe$_2$O$_3$ or Fe$_3$O$_4$. Their superparamagnetic magnetization is much higher than that for normal paramagnetic materials and it can reach approximately the magnetization saturation of ferromagnetic iron oxide. Importantly, after elimination of the magnetic field, SPIONs are no longer magnetized.[1-,2, 3] This feature has made them the subject of increased scientific interest. There are number of reports on their applications *in vivo*, such as T_2 contrast agents in magnetic resonance imaging (MRI), detoxification of biological fluids, in hyperthermia, tissue repair, cell separation etc.[4-, 5,6,7,8,9] Unfortunately, SPIONs may undergo aggregation, which implies changes in their magnetic properties and may lead to their unwanted fast elimination from the circulatory system. Formation of a protective coatings is one of the methods used for their stabilization in suspension.[10] It has been proven, that the formation of polymer coatings on SPIONs can prevent their aggregation and improve their biocompatibility and stability.[11,12]

We have only recently shown that application of cationic derivative of chitosan (CCh[13] during the formation of nanoparticles via co-precipitation from aqueous ammonia solution of iron salts results in coating of SPIONs with that polymer. The nanoparticles are stably enwrapped since the polymer is introduced during formation of the nanoparticles but not in post processing that may suffer from aggregation of naked nanoparticles prior coating. Since CCh contains quaternary ammonium salts the charge of such formed SPIONs is positive at neutral and even basic pH. That coating improved stability of the nanoparticles' aqueous dispersion, resulted in high relaxivity value, which is an important parameter for MRI contrast agents, [14,15] and provided the opportunity for further modification of their surfaces via coating them using LbL method. [16] We have already demonstrated that in our previous reports using anionically modified chitosan what allowed us to prepare the negatively charged SPIONs,[14] and bimodal contrast agents containing Gd ions shortening T_1 relaxation time.[17] Such multimodal systems have attracted increasing interest in development of molecular imaging and in theranostics.[18-,19,20,21] Bimodal imaging agents serving both for MRI and fluorescence imaging are of special interest.

In the current paper we report on fabrication and characterization of novel bimodal SPIONs coated with hyaluronic acid (HA) derivative containing curcumin as a fluorescent dye that can serve as contrast agent for both MRI and fluorescence imaging. Hyaluronic acid (HA), a naturally occurring polysaccharide composed of N-acetyl-D-glucosamine and D-glucuronic acid, has a strong negative charge. Moreover, HA was shown to have affinity for the cell-specific surface markers such as CD44 and RHAMM. [22,23] Thus, the cancer cells with high metastatic activities often exhibit enhanced binding and uptake of HA. [24] Curcumin is a natural polyphenol obtained from the rhizomes of turmeric (*Curcuma longa*). This yellow dye, in addition to fluorescent properties, shows a variety of desired pharmacological properties, including anti-inflammatory, anti-cancer and anti-oxidant activities.[25-,26,27,28] In this report we fabricated and tested SPIONs with curcumin embedded in the cores of the nanoparticles as well as present in their thin polymeric coatings.

2. Materials and methods

2.1. Materials

Hyaluronic acid sodium salt (HA), curcumin (≥94% (curcuminoid content), ≥80%)), N,N-dicyclohexylcarbodiimide (DCC), 4-dimethylaminopyridine (DMAP), dimethylsulfoxide

(puriss p.a., 0.02% water) (DMSO), iron(III) chloride hexahydrate, iron(II) chloride tetrahydrate (all from Sigma-Aldrich, USA), tetraethoxysilane (TEOS, P98%, Fluka), ethanol (99.8%, spectroscopic grade, Chempur, Poland) and ammonium hydroxide (25%, pure p.a., Chempur) were used as received. Cationic derivative of chitosan, N-[(2-hydroxy-3-trimethylammonium) propyl] chitosan chloride (CCh), was synthesized and characterized according to the procedures described earlier[13] using low molecular weight chitosan (Sigma-Aldrich). Anionic derivative of chitosan (ACh) was synthesized and characterized according to the procedures described earlier.[14] Deionized water was used for all the experiments.

2.2. Synthesis of hyaluronic acid–curcumin conjugate (HA-Cur)

DCC (50 mg) and DMAP (20 mg) were added to the solution of HA (400 mg) in DMSO (100 mL). The mixture was stirred for 1h under nitrogen atmosphere, to activate carboxylic groups of HA. Then 20 mL of 0.1 mM solution of curcumin in DMSO was slowly added to that mixture. The resulting solution was stirred for 8h at 60ºC. The mixture was then dialyzed against DMSO for 24h and then against deionized water for 9 days using a dialysis membrane (MWCO: 12 kDa) to remove unbound residues. The resulting product, HA-Cur conjugate was then lyophilized.

2.3. Preparation of SPION-CCh-Cur

The synthesis of SPIONs containing embedded curcumin (SPION-CCh-Cur) was carried out in an aqueous solution. At first, iron salts, in molar ratio Fe(III): Fe(II) = 2:1, (0.1622 g $FeCl_3 \cdot 6H_2O$ and 0.0596 g $FeCl_2 \cdot 4H_2O$), were dissolved in 50 mL of aqueous solution of CCh (c = 3 g/L) that pH value of ca. 1.5. The solution was deoxygenated by purging with argon and sonicated (Sonic-6, Polsonic, 480 W, 1s pulse per every 5s) for 10 min in a thermostatic bath at 20°C. During the sonication, 100 μL of the curcumin solution in ethanol (1 g/L) was added. After that, 5 mL of 5 M $NH_{3(aq)}$ solution was added dropwise and the mixture was further sonicated for 30 min. The obtained suspension was filtered through the cellulose syringe filter with 0.2μm pore diameter. Purification of the formed SPIONs was performed using magnetic chromatography described elsewhere.[14]

2.4. Preparation of SPION-CCh-Cur coated by HA-Cur conjugate

The synthesized positively charged SPION-CCh-Cur were coated with the anionic HA-Cur conjugate using "layer-by-layer" deposition method. Aqueous solution of HA-Cur (10 mL, c

= 1 g L^{-1} in 0.1 M NaCl) was added to the suspension of SPION-CCh-Cur (4 mL) and sonicated continuously for 10 min at 25°C. The obtained SPION-CCh/HA-Cur nanoparticles were purified using magnetic chromatography.

2.5. Preparation of SPION-CCh and SPION-CCh/ACh

The positively charged SPION-CCh and negatively charged SPION-CCh/ACh were obtained according to the procedure described earlier.[14] Briefly, the aqueous solution of anionic chitosan (ACh) (10 mL, c = 1 g L^{-1} in 0.1 M NaCl) was added to the suspension of SPION-CCh (4 mL) and sonicated continuously for 10 min at 25°C. The coated nanoparticles were purified using magnetic chromatography.

2.6. Apparatus

Absorption and emission spectra measurements

Electronic absorption spectra were measured at 25°C using Hewlett-Packard 8452A diode-array spectrophotometer, equipped with HP 89090A Peltier temperature control accessory. Fluorescence emission spectra were measured using PerkinElmer LS55 fluorescence spectrometer at 25°C. Quartz cuvettes of 1 cm optical path length (Hellma) were used for all the measurements.

Dynamic light scattering (DLS) and zeta potential measurements

A Malvern Nano ZS light-scattering apparatus (Malvern Instruments Ltd., Worcestershire, UK) was used for dynamic light scattering (DLS) and zeta potential measurements. The time-dependent autocorrelation function of the photocurrent was acquired every 10s (15 acquisitions for each run). The sample was illuminated by a 633-nm laser and the intensity of light scattered at an angle of 173° was measured by an avalanche photodiode. The z-average hydrodynamic mean diameters and distribution profiles of the samples were calculated using the software provided by Malvern. The zeta potential was measured using laser Doppler velocimetry (LDV) method provided by Nano ZS instrument.

Magnetic properties of SPIONs

To study the magnetic properties of the obtained nanoparticles, magnetic hysteresis curves were obtained using vibrating sample magnetometer VSM-NUVO (Molspin Ltd., Newcastle-on-Tyne, England). Relaxivities were measured on MiniSpec mq-20 (20MHz) and MiniSpec mq-60 (60MHz) (Bruker, Ettlingen, Germany), and nuclear magnetic relaxation dispersion

(NMRD) profiles were acquired on Spinmaster-FFC 2000 relaxometer (Stelar s.r.l., Mede, Italy). The relaxivity measurements and calculation were performed following the procedure previously reported by us.[14]

Confocal fluorescence microscopy of SPIONs-loaded cells

Murine fibroblasts (NIH3T3) cell line was cultured in DMEM high glucose medium in a humidified incubator under standard conditions (37°C, 5% CO2). The cells prior the fluorescence measurements were incubated in the suspension of SPIONs (1 μM concentration of iron) in DMEM with 10 % fetal bovine serum (FBS) for 24h. The cells were then washed twice with phosphate buffer solution PBS (pH=7.4) and fixed with 1% paraformaldehyde in PBS for 15 min at 4°C. Confocal fluorescence imaging of the cells was performed using a Nikon Ti-E inverted microscope equipped with a Nikon A1 confocal system. For the excitation a 405 nm diode laser was used. The images were acquired in the emission mode with a Plan Apo 100×/1.4 Oil DIC objective. In order to remove the fluorescence background originating from the cells a 458 nm barrier emission filter was applied. The resolution of the images was 2048×2048 pixels.

Other measurements

The elemental analysis (C, H, and N) was performed with a EuroEA 3000 analyzer. FT-IR spectra were measured using a Bruker IFS 48 spectrometer. NMR spectra were measured in DMSO-d^6 using a Bruker AMX 500 spectrometer. Gel permeation chromatography (GPC) analyses were performed using a Waters GPC system equipped with a set of three columns (PL Aquagel-OH 30, 40, and 60) and tandem PDA/RI detectors.

2.7. Cytotoxicity studies

Viability of EA.hy926 endothelial cells treated with SPIONs was evaluated by Trypan blue method following the procedure described in Trypan blue exclusion protocol in Thermo Fisher Scientific web page. The cells were grown in 24 well plates for 48 h in the presence of 10% FBS in the medium. Subsequently, the medium was replaced with a serum-free medium containing appropriate SPIONs (15 μg/ml) and the cells were cultured for additional 24 h. Then, viability assay was performed and the samples were immediately investigated using optical microscope (Olympus IX71). About 30 images were taken for every sample in order to count viable and dead cells. Cell viability was presented as percentage of viable cells in the

population of cells. Each experiment was repeated three times and the data were presented as mean ± SD.

3. Results and discussion

Polymeric coating can significantly alter stability and physicochemical properties of nanoparticles. Thus, in addition to fabrication of cationic SPIONs containing embedded curcumin (SPION-CCh-Cur), the nanoparticles were also coated by an anionic polysaccharide, hyaluronic acid, that was additionally modified by conjugation with curcumin, which serves as a fluorophore. Hyaluronic acid–curcumin conjugate (HA-Cur, see Figure S1 in Supporting Information) was synthesized by esterification reaction, which was carried out according to the Steglich mechanism.[29] Preparation of the conjugate was possible due to the presence of reactive carboxyl groups in hyaluronic acid and hydroxyl groups in curcumin molecules. The formation of HA-Cur conjugate was confirmed using FT-IR and ^{1}H NMR spectrosocpies (see Fig. S2 and S3 in SI).

3.1. The effect of curcumin and HA-Cur coating on size and zeta potential of SPION-CCh

The size and morphology of the obtained SPIONs were determined by transmission electron microscopy (TEM). The images showed well-separated nanoparticles within small aggregates (Figure S4 in SI). The core sizes of SPION-CCh were found to be very small, with an average diameter of 11.9 ± 1.7 nm. Embedding of curcumin into the nanoparticles did not cause a significant change in their sizes. The average core size of SPION-CCh-Cur was found to be about $d = 10.1 \pm 2.9$, that is very similar to the size of SPION-CCh.

DLS measurements have shown that the nanoparticles form small aggregates in an aqueous dispersion. The hydrodynamic diameter and zeta potential of SPIONs were found to be equal to 112 ± 2 nm and $+28 \pm 5$ mV, respectively. Embedding curcumin to SPIONs caused slight increase of zeta potential to $+35 \pm 1$ mV although the hydrodynamic size remained almost unchanged (see Table 1). The nanoparticles appeared to be stable also in PBS at pH=7.4 that is typically used for cell culturing. The moduli of measured zeta potential values slightly decreased (see Table 1) but it is not surprised as those values normally decrease with increasing ionic strength of solutions.

7

Coating of the nanoparticles with HA-Cur polyanion changed the zeta potential of SPIONs from +35 to -31 mV (see Table 1). It can be seen that SPION-CCh/HA-Cur form smaller aggregates which size was about 50 nm (Figure S5 in SI) indicating their better stabilization in an aqueous dispersion in comparison to the uncoated SPION-CCh.

3.2. Relaxometric properties of SPIONs

The spin lattice relaxation (NMRD) profiles of the obtained SPIONs are shown in Figure 1. NMRD profiles for all the studied systems have the shape typical for superparamagnetic nanoparticles with decreasing trends in the high-frequency part. Generally, for colloidal magnetic nanoparticles, the shape of the NMRD profile is determined by crystallinity and size of magnetic cores (as they affect saturation magnetization), availability of solvent molecules to the cores (diffusion) and interactions between the magnetic cores (anisotropy energy effect).[11] The measured profiles indicated that the overall sizes of nanoparticles increase after covering them with the HA-Cur layer. Furthermore, increase in the size of nanoparticles produced systematic changes in the magnetic resonance properties of the samples. The NMRD data demonstrated that values of relaxivity, r_1, increased when the diameter of the nanoparticles increased, especially in the low-frequency region of the profiles. The values of magnetization saturation and particle diameters obtained by fitting to the theoretical equation[30] to the experimental data are listed in Table 2.

The diameters of SPIONs obtained from TEM images are smaller than those obtained from fitting NMRD profiles. This discrepancy may be explained by the fact that the diameters calculated from relaxometry measurements take into account also water molecules present around the magnetic core. Chemical nature and thickness of the coating play important roles in relaxometry and give contributions to the calculated diameter of nanoparticles while TEM can hardly see the organic coating on the magnetic cores. Thus, the relaxometry data indicate effective covering of magnetic cores by polymeric materials.

The efficacy of SPION as MRI contrast agents is related to their r_1 and r_2 relaxivity values (see Table 3). Relaxivities are reported with respect to the total molarity of iron.

The high values of relaxivity obtained for the SPIONs systems could be partially explained by the effect of aggregation of small nanoparticles[15] but the effect of high hydration of the nanoparticle coatings as it was postulated by Haan and Paquet[31] seems to be dominating. Here, we used highly charged polymers (HA-Cur, CCh, ACh) for coating the nanoparticles. For these coatings, one can expect high hydration, but slower diffusion of water molecules in the presence of the SPIONs within the hydrophilic polymer layers. Such decrease in water diffusion coefficients in polysaccharides was previously observed by Kwak and Lafleur. [32] These explanations are in line with the observation of significant increase of r_2 value (Table 3) after deposition of HA-Cur on SPION-CCh without any change in the inorganic core of the nanoparticles and with only small change in the average size of the aggregates. The similar effect was observed by us earlier[14,15] for SPIONs coated with ultrathin layer of anionic derivatives of chitosan (ACh). However, the value of relaxivity r_2 for SPION-CCh/HA-Cur system (ca. 470 $mM^{-1} \cdot s^{-1}$ at 20 MHz) was significantly higher than that one found for SPION-CCh/ACh. It indicates that SPION-CCh/HA-Cur may be particularly attractive as T_2 contrast agent for MRI.

3.3. Fluorescent properties of SPIONs

The fluorescence characteristics of the obtained hybrid materials are shown in Figure 2. SPION-CCh-Cur containing curcumin introduced at the stage of their synthesis show only very weak fluorescence band with maximum near λ = 550-570 nm (λ_{ex} = 405 nm). The maximum of this band is shifted to longer wavelengths as compared to methanol-water solution of curcumin. That shift may be explained by the formation of complexes between curcumin and Fe^{3+} ions. [33,34] For SPION-CCh-Cur/HA-CUR much more intensive fluorescence band, in the range characteristic of curcumin, was observed. As expected, the aqueous dispersion of SPION-CCh was not fluorescent at all.

Cellular uptake and the location of nanoparticles in NIH3T3 fibroblasts cells were investigated using scanning laser fluorescence confocal microscopy. The studies were based on the detection of nanoparticles by observation of characteristic curcumin fluorescence (excitation at 408 nm and emission at 480-540nm). Figure 3B shows cellular uptake and localization of SPION-CCh-Cur in cells and Figure 3C present the respective image for SPION-CCh/HA-Cur, both after 24h of incubation. In comparison to control system (Figure

9

3A) both systems show green emission characteristic of curcumin indicating that the nanoparticles were uptaken by the cells. Figure 3C shows much more intense green emission than Figure 3B but both significantly differ from the control cells (Figure 3A). Furthermore, for the sample treated with SPION-CCh-Cur, already after 1 minute of exposure on light, fluorescence intensity significantly decreased. Based on these observations it can be concluded that both the obtained dual modality SPIONs were effectively delivered to NIH3T3 cells. However, the SPIONs coated with HA-Cur are characterized by more intense fluorescence and higher photostability that may be explained by formation of micellar structures by the conjugate protecting HA from contact with water. [35]

3.4. Cytotoxicity studies

Considering potential biomedical applications of the obtained SPION-CCh/HA-Cur it was essential to determine their cytotoxicity and compare with the uncoated cationic SPION-CCh. Thus, the viabilities of the selected endothelial EA.hy926 cells treated with the mentioned SPION systems were determined. These cells, more sensitive than fibroblasts used here in SPION uptake studies, were chosen in order to bring more conclusive results of cytotoxicity studies. EA.hy926 cells viability was evaluated by the Trypan blue method. The results presented in Figure 4 indicate that the studied SPIONs exhibit significantly different levels of cytotoxicity to the model cells. The test confirmed that SPION-CCh exhibited considerable cytotoxicity towards EA.hy926 cells, decreasing their viability to ca. 70% of the control system. This decrease in the cell viability is likely caused by the presence of cationic groups on the SPION-CCh surface. It is known that cationic derivatives of chitosan (containing quaternary ammonium groups) can be cytotoxic to various types of cells. [36,37] However, no toxic effect was observed when cells were exposed to SPION-CCh/HA-Cur at the same 1 μM concentration.

4. Conclusions

Biocompatible superparamagnetic iron oxide nanoparticles (SPIONs) coated with ultrathin layer of cationic derivative of chitosan and hyaluronic acid - curcumin conjugate (SPION-CCh/HA-Cur) were prepared in a simple water-based two-step procedure. The core size of the nanocoated SPIONs was slightly above 10 nm, while hydrodynamic diameter of the hydrated aggregates of nanoparticles in aqueous dispersion was ca. 50 nm, and the zeta potential was about -31 mV. The electrostatic repulsion between particles ensured stability of their aqueous

dispersion. The magnetic properties with very high values of saturation magnetization (43.4 ± 0.2 emu g^{-1} Fe) and transverse relaxivity (469.7 ± 2.3 mM^{-1} s^{-1}) for SPION-CCh/HA-Cur, indicate that they could be considered for applications as MRI contrast agents. Biological studies indicated that SPION-CCh/HA-Cur can be easily internalized into the cells and they do not show cytotoxicity at the applied concentration. Due to the high efficiency of the curcumin fluorescence the obtained SPION-CCh/HA-Cur can be treated as bimodal probes useful for studies of the biological objects using both MRI and fluorescence detection.

References

[1] R. Kaiser, G. Miskolcz, Some applications of ferrofluid magnetic colloids, IEEE Trans. Magnetics MAG-6 (3) (1970) 694-698.

[2] T. Sugimoto, E. Matijevic, Formation of uniform spherical magnetite particles by crystallization from ferrous hydroxide gels, J. Colloid. Interface Sci.74 (1980) 227–243.

[3] H. Itoh, T. Sugimoto, Systematic control of size, shape, structure, and magnetic properties of uniform magnetite and maghemite particles, J. Colloid. Interface Sci. 265 (2003) 283-95.

[4] A. K. Gupta, M. Gupta: Synthesis and surface engineering of iron oxide nanoparticles for biomedical applications, Biomaterials 26 (2005) 3995–4021.

[5] O. Kaman, E. Pollert, P. Veverka, M. Veverka, E. Hadová, K. Knížek, M. Maryško, P. Kašpar, M. Klementová, V. Grünwaldová, S. Vasseur, R. Epherre, S. Mornet, G. Goglio, E. Duguet, Silica encapsulated manganese perovskite nanoparticles for magnetically induced hyperthermia without the risk of overheating, Nanotechnology 20 (2009) 2756101–2756107.

[6]   K.S. Park, J. Tae, B. Choi, Y.S. Kim, S.H. Kim, H.S. Lee, J. Kim, J. Kim, J. Park, J.H. Lee, J.E. Lee, J.W. Joe, S. Kim, Characterization, in vitro cytotoxicity assessment, and in vivo visualization of multimodal, RITC-labeled, silica-coated magnetic nanoparticles for labeling human cord blood–derived mesenchymal stem cells, Nanomedicine. 6 (2010) 263–276.

[7]   J. Yang, J. Gunn, S.R. Dave, M. Zhang, Y.A. Wang, X. Gao, Ultrasensitive detection and molecular imaging with magnetic nanoparticles, Analyst 133 (2008) 154–160.

[8]   T. Neuberger, B. Schöpf, H. Hofmann, M. Hofmann, B. Rechenberg, Superparamagnetic nanoparticles for biomedical applications: Possibilities and limitations of a new drug delivery system, J. Magn. Magn. Mater. 293 (2005) 483–496.

[9]   C.H. Cunningham, T. Arai, P.C. Yang, M.V. McConnell, J.M. Pauly, S.M. Conolly, Positive contrast magnetic resonance imaging of cells labeled with magnetic nanoparticles, Magn. Reson. Med. 53 (2005) 999–1005.

[10]   D.K. Kim, M. Mikhaylova, Y. Zhang, M. Muhammed, Protective Coating of Superparamagnetic Iron Oxide Nanoparticles, Chem. Mater. 15(2003) 1617-1627.

[11]   S. Laurent, D. Forge, M. Port, A. Roch, C. Robic, L. Vander Elst, R.N. Muller, Magnetic Iron Oxide Nanoparticles: Synthesis, Stabilization, Vectorization, Physicochemical Characterizations, and Biological Applications, Chem. Rev. 108 (2008) 2064–2110.

[12]   Lu Z, Dai J, Song X, Wang G, Yang W, Facile synthesis of Fe3O4/SiO2 composite nanoparticles from primary silica particles, Colloids Surf. A, 317 (2008) 450-456.

[13]   M. Bulwan, S. Zapotoczny, M. Nowakowska, Robust one component chitosan-based ultrathin films fabricated using layer-by-layer technique, Soft Matter 5 (2009) 4726–4732.

[14]   A. Szpak, G. Kania, T. Skórka, W. Tokarz, S. Zapotoczny, M. Nowakowska, Stable aqueous dispersion of superparamagnetic iron oxide nanoparticles protected by charged chitosan derivatives, J. Nanopart . Res. 15 (2013) 1372.

[15]   T. Panczyk, Ł. Konczak, S. Zapotoczny, P. Szabelski, M. Nowakowska, Molecular dynamics simulations of proton transverse relaxation times in suspensions of magnetic nanoparticles, J. Colloid Interface Sci. 437 (2015) 187–196.

[16]   C. Picart, F. Caruso and J.-C. Voegel (Eds.), Layer-by-Layer Films for Biomedical Applications, Wiley-VCH, Weinheim, 2015.

[17] A. Szpak, S. Fiejdasz, W. Prendota, T. Strączek, C. Kapusta, J. Szmyd, M. Nowakowska, S. Zapotoczny, T1–T2 Dual-modal MRI contrast agents based on superparamagnetic iron oxide nanoparticles with surface attached gadolinium complexes. J. Nanopart . Res. 16 (2014) 2678.

[18] R. Thomas, I.K. Park, Y.Y. Jeong, Magnetic iron oxide nanoparticles for multimodal imaging and therapy of cancer, Int. J. Mol. Sci. 14 (2013) 15910-15930.

[19] H. Fattahi, S. Laurent, F. Liu, N. Arsalani, L. Vander Elst, R.N.Muller, Magnetoliposomes as multimodal contrast agents for molecular imaging and cancer nanotheragnostics, Nanomedicine 6 (2011) 529-544.

[20] M. J. Janjic, P. Shao, Z. Shaojuan, Y. Xun, K.P. Sravan, M. Bai, Perfluorocarbon nanoemulsions with fluorescent, colloidal and magnetic properties, Biomaterials 35 (2014) 4958-4968.

[21] A. Housni, S. Boujraf, Multimodal magnetic resonance imaging in the diagnosis and therapeutical follow-up of brain tumors, Neurosciences 18 (2013) 3-10.

[22] H. Maeda, L.W. Seymour, Y. Miyamoto, Conjugates of Anticancer Agents and Polymers: Advantages of Macromolecular Therapeutics in Vivo, Bioconjugate Chem. 3 (1992) 351–362.

[23] P. Herrlich, J. Leeman, D. Wainwright, H. Konig, L. Sherman, H. Ponta, How Tumor Cells Make Use of CD44, Adhes. Commun. 6 (1998) 141–147.

[24] C.L. Hall, B. Yang, X. Yang, S. Zhang, M. Turley, S. Samuel, L.A. Lange, C. Wang, G.D. Curpen, R.C. Savani, A.H. Greenburg, E.A. Turley, Overexpression of the hyaluronan receptor RHAMM is transforming and is also required for H-ras transformation, Cell 82 (1995) 19–28.

[25] D. Karunagaran, R. Rashmi, T.R. Kumar, Induction of apoptosis by curcumin and its implications for cancer therapy, Curr. Cancer Drug Targets 5 (2005) 117-129.

[26] B.B. Aggarwal, C. Sundaram, N. Malani, H. Ichikawa, Curcumin: the Indian solid gold, Adv. Exp. Med. Biol. 595 (2007) 1-75.

[27] J.L. Ji, X.F. Huang, H.L. Zhu, Curcumin and its formulations: potential anti-cancer agents, Anti-Cancer Agents Med. Chem. 12 (2012) 210–218.

[28] B. Tharakan, F.A. Hunter, W.R. Smythe, E.W. Childs, Curcumin inhibits reactive oxygen species formation and vascular hyperpermeability following haemorrhagic shock, Clin. Exp. Pharmacol. Physiol. 37 (2010) 939-944.

[29] B. Neises, W. Steglich, Simple Method for the Esterification of Carboxylic Acids, Angew. Chem. Int. Ed. 17 (1978) 522-524.

[30] A. Roch, R. N. Muller, P. Gillis, Theory of proton relaxation induced by superparamagnetic particles, J. Phys. Chem. 110 (1999) 5403-5411.

[31]   H.W. De Haan, C. Paquet, Enhancement and degradation of the R2* relaxation rate resulting from the encapsulation of magnetic particles with hydrophilic coatings, Magn. Reson. Med. 66 (2011) 1759-1766.

[32]   S. Kwak, M. Lafleur, NMR self-diffusion measurements of molecular and macromolecular species in dextran solutions and gels, Macromolecules 36 (2003) 3189–3195.

[33]   M. Borsari, E. Ferrari, R.Grandi, M. Saladini, Curcuminoids as potential new iron-chelating agents: spectroscopic, polarographic and potentiometric study on their Fe(III) complexing ability, Inorg. Chim. Acta 328 (2002) 61–68.

[34]   M. Bernabé-Pineda, M.T. Ramírez-Silva, M.A. Romero-Romo, E. González-Vergara, A. Rojas-Hernández, Spectrophotometric and electrochemical determination of the formation constants of the complexes Curcumin-Fe(III)-water and Curcumin-Fe(II)-water, Spectrochim. Acta A Mol. Biomol. Spectrosc. 60 (2004) 1105-1113.

[35]   S. Manju, K. Sreenivasan, Conjugation of curcumin onto hyaluronic acid enhances its aqueous solubility and stability, J. Colloid Interf. Sci. 359 (2011) 318–325.

[36]   B. Xiao, Y. Wan, X. Wang, Q. Zha, H. Liu, Z. Qiu and S. Zhang, Synthesis and characterization of N-(2-hydroxy)propyl-3-trimethyl ammonium chitosan chloride for potential application in gene delivery, Colloids Surf. B 91 (2012) 168–174.

[37] G. Kania, U. Kwolek, K. Nakai, S-I.Yusa, J. Bednar, T. Wójcik, S. Chłopicki, T. Skórka, M. Szuwarzyński, K. Szczubiałka, M. Kepczynski, M. Nowakowska, Stable polymersomes based on ionic-zwitterionic block copolymers modified with superparamagnetic iron oxide nanoparticles for biomedical applications, J. Mater. Chem. B 27 (2015) 5523-5531.
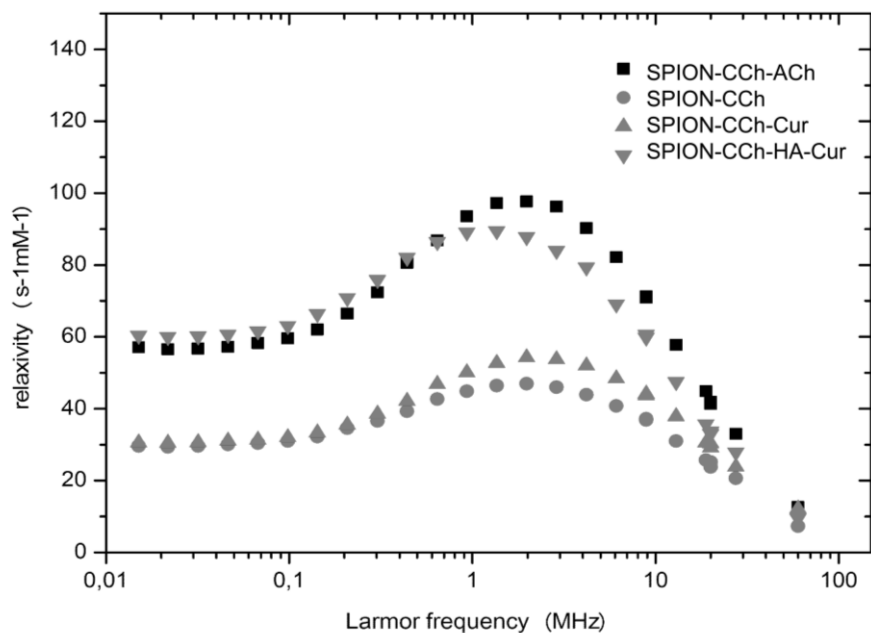
Figure 1. Proton NMRD profiles of SPION-CCh, SPION-CCh/ACh, SPION-CCh-Cur and SPION-CCh/HA-Cur in water at 37 °C.
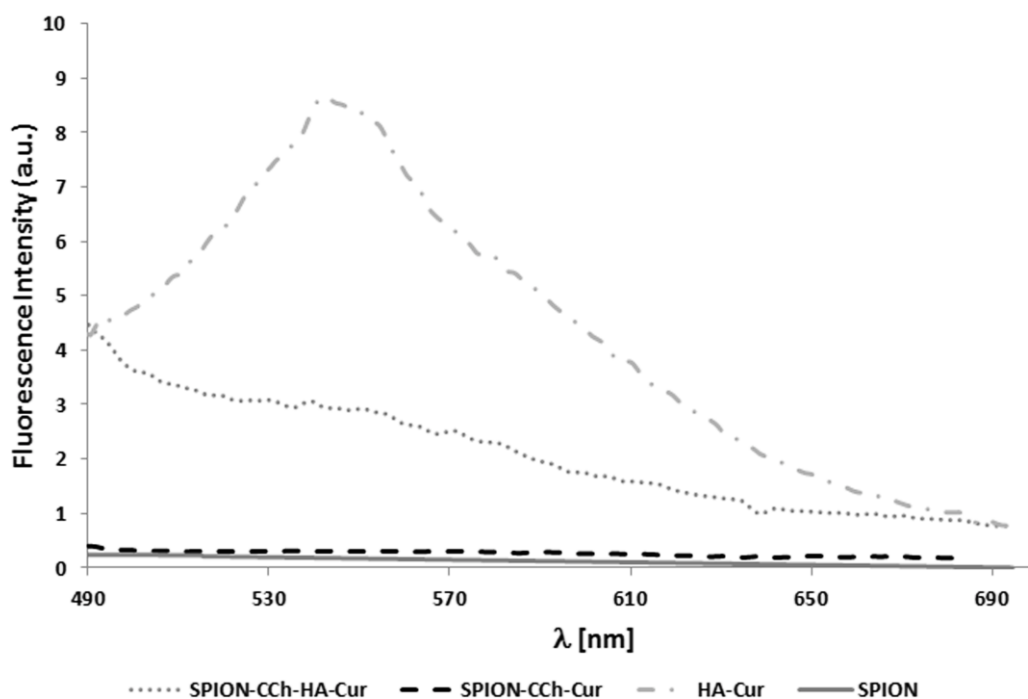
Figure 2. Fluorescence spectra of nanoparticles (λ_{ex} = 405 nm) (SPION-CCh, SPION-CCh-Cur, SPION-CCh-Cur/HA-Cur) in aqueous dispersions (c = 0.2 mM) and aqueous solution of conjugate HA-Cur (c = 0.2 g L^{-1}).
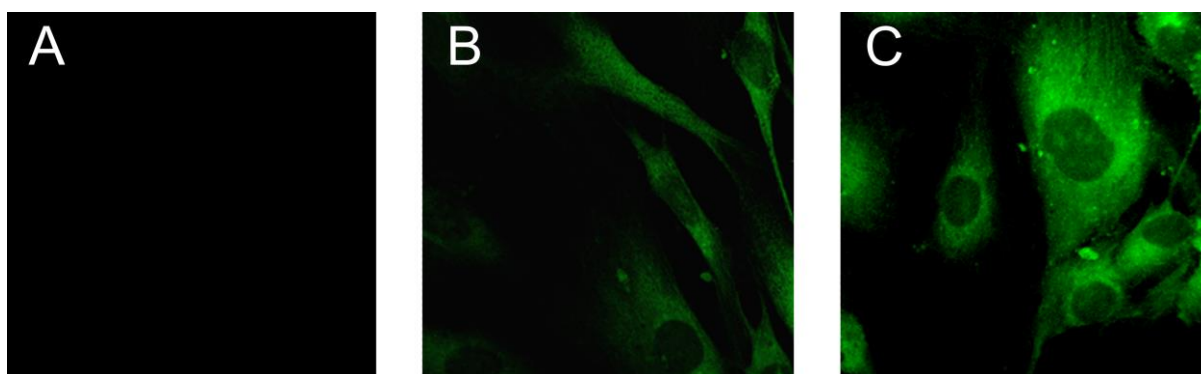
Figure 3. Confocal fluorescence images of fibroblasts cells recorded before (A) and 24h after treatment with (B) SPION-CCh-Cur (1 μM) and (C) SPION-CCh/HA-Cur (1 μM).
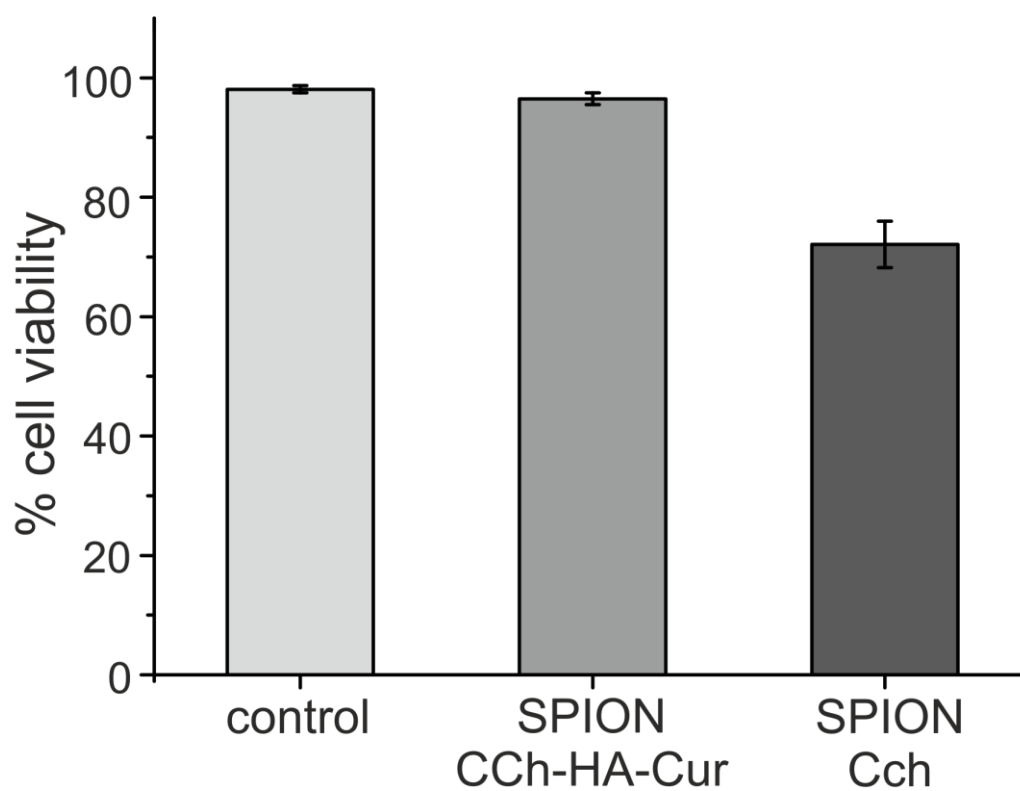
Figure 4. Effect of different SPION systems on the viability of EA.hy926 cells. Values represent the mean ± SD of triplicate experiments (n = 3) after 24 h of exposure to various SPIONs (1 μM).

Table 1 Values of the mean hydrodynamic diameter (measured by DLS) and zeta potential of obtained SPIONs in water and PBS. Data are expressed as mean ± SD (n=3).

Type of SPIONs	Hydrodynamic diameter (nm)	Zeta potential (mV)
SPION-CCh	112 ± 2	+28 ± 5 (+11± 1)[a]
SPION-CCh/ACh	92 ± 7	-51 ± 2
SPION-CCh-Cur	108 ± 2	+35 ± 1 (+14± 1)[a]
SPION-CCh/HA-Cur	46 ± 5	-31 ± 1 (-24 ± 2)[a]

[a] Measured in PBS

Table 2 Values of saturation magnetization and mean diameters of magnetic cores as determined using magnetic measurements. Data are expressed as mean ± SD (n=4).

Sample	Saturation magnetization M_{sat} [Am²/kg]	Diameter [nm]
SPION-CCh	37.1 ± 0.2	16.3 ± 0.1
SPION-CCh/ACh	48.8 ± 0.2	17.4 ± 0.1
SPION-CCh-Cur	42.5 ± 0.2	15.3 ± 0.1
SPION-CCh/HA-Cur	43.4 ± 0.2	18.4 ± 0.1

Table 3 Relaxivity values of SPIONs at 37°C for selected frequencies: 20 MHz and 60 MHz. Data are expressed as means ± SD (n=4).

Sample	20 MHz			60 MHz		
	r_1 [s⁻¹·mM⁻¹]	r_2 [s⁻¹·mM⁻¹]	r_2/r_1	r_1 [s⁻¹·mM⁻¹]	r_2 [s⁻¹·mM⁻¹]	r_2/r_1
SPION-CCh	23.8±0.1	173.8±0.1	7.3	7.3±0.1	172.3±0.1	23.5
SPION-CCh/ACh	41.3±0.3	361.3±0.9	8.7	12.6±0.1	386.5±0.3	30.6
SPION-CCh-Cur	30.4±0.2	182.4±0.5	6.0	12.1±0.1	196.5±3.4	16.1
SPION-CCh/HA-Cur	33.1±0.1	469.7±2.3	14.2	9.5±0.1	497.2±0.4	52.1